ELSEVIER

International Journal of Pharmaceutics 131 (1996) 209–217

international journal of pharmaceutics

Holographic evaluation of bending and integrity of pharmaceutical powder beams

Raimo Silvennoinen[a], Pasi Raatikainen[b,*], Jarkko Ketolainen[b], Pertti Ketolainen[a], Petteri Paronen[b]

[a] *Väisälä Laboratory, Department of Physics, University of Joensuu, P.O. Box 111, FIN-80101 Joensuu, Finland*
[b] *Department of Pharmaceutical Technology, University of Kuopio, P.O. Box 1627, FIN-70211 Kuopio, Finland*

Received 27 February 1995; revised 5 September 1995; accepted 24 September 1995

Abstract

Double-exposure holographic interferometry was used to detect structural uniformity and bending properties of compressed rectangular beams consisting of microcrystalline cellulose, dicalcium phosphate dihydrate and α-lactose monohydrate. The fringes in holographic reconstructions produced a clear pattern for interpretation of bending without any complication. Thus, it was possible to calculate the elastic modulus values for both the upper and lower surfaces of the sample beams. The theoretical bending profiles versus experimental bending data were also evaluated. It was possible to detect unpredictable changes due, for example, to structural non-homogeneities and induced stress. The induced stress inside the beams had a slight effect on the ideal bending, due to the fixing of the beam. The modulus values obtained from extrapolation to zero porosity were in good agreement with the previously published results. According to this study, double-exposure holographic interferometry is a suitable, accurate and versatile method for mechanical studies of pharmaceutical powders and compacts.

Keywords: Pharmaceutical powders; Elastic deformation; Beam bending; Double-exposure holographic interferometry; Young's modulus; Specimen integrity

1. Introduction

Deformation properties essentially affect the compactibility and compressibility of pharmaceutical powders. The most important properties include the tendency to undergo plastic flow, brittle fracture, as well as elastic deformation and recovery. Elastic properties result from the elastic deformation of particle surfaces, due to reversible slipping of crystal planes, and from less specific elasticities of particles consisting of less oriented, or even amorphous materials. In both cases, the elasticity is dependent on the equilibrium of attractive and repulsive inter- and intramolecular forces (Roberts et al., 1991). The second type of elastic phenomena is the dimensional recovery of the compact. Besides the intrinsic elasticity of the materials, this is also dependent on the different mechanical and thermophysical interactions inside the heterogeneous, disperse powder-air compact (Bassam et al., 1988, 1990; Roberts et al., 1993).

* Corresponding author.

SSDI 0378-5173(95)04329-Z

Elastic properties of pharmaceutical powders are typically evaluated by energy consumption calculations (Roberts et al., 1991), testing of compact's surface hardness using an indenter (Roberts and Rowe, 1987; Holman and Leuenberger, 1988; Sinko et al., 1992), or dimensional recovery measurements after compaction (Dwivedi et al., 1992). Also, bending tests have recently gained in popularity (Church and Kennerley, 1984; Mashadi and Newton, 1987; Bassam et al., 1988, 1990). The beam bending tests allow for the calculation of Young's modulus values for intact solid material, i.e. extrapolated into the zero porosity state (Bassam et al., 1991; Roberts et al., 1991). These tests are performed with a series of compressed specimens, typically rectangular beams, with a wide porosity range. Although experimental difficulties exist, this procedure can be used for obtaining a numerical parameter that describes the intrinsic tendency of pharmaceutical materials to undergo elastic deformation (Raatikainen et al., 1994). Difficulties exist especially in the preparation of even, homogeneous beams having a sufficiently dense structure. Also, the accuracy of the beam bending apparatus is often too limited for detecting small dimensional changes. Strain measurement is typically performed using either mechanical displacement transducers (e.g. LVDTs) or potentiometric detectors. These methods typically allow for only the observation of localized displacement (i.e. bending in one specific point along the beam length, and not the displacement profile of the whole beam).

This study evaluates the structural uniformity and bending properties of some pharmaceutical powders by an optical measurement. The method applied was double-exposure holographic interferometry, which is based on a recording of two successive exposures on the same holographic plate (Dhir and Sikora, 1972; Pryputniewicz and Bowley, 1978). The aims also included an evaluation of this method and bending setup for clear interpretation, and evaluation of bending both the upper and lower surfaces of the sample beams. Compacted rectangular beam specimens, consisting of microcrystalline cellulose, dicalcium phosphate dihydrate or α-lactose monohydrate, were examined using the cantilever beam bending method.

2. Materials and methods

2.1. Beam preparation

The materials used in this study for the preparation of beam specimens were microcrystalline cellulose, (Avicel® PH 101, FMC, USA), dicalcium phosphate dihydrate, (Emcompress®, E. Mendell, USA), and α-lactose monohydrate (sieve fraction 149–210 μm, DMV, Holland). The materials were stored for at least 2 weeks under a relative humidity of 45% prior to compaction of the rectangular beam specimens, and after compaction for at least 5 days under the same storage conditions, before testing. All test materials were compressed using a hardened steel punch and die set, giving a beam sample size of 60 × 6 × 2 mm. Thicknesses of the beams were adjusted using rejector plates, which stopped the punch movement so that the thickness was 2.0 ± 0.1 mm. Beams were prepared by varying the weight of the powder in the die. Compression of the sample beam was made to different porosities without any structural failures (e.g. lamination or cracks) visible to the naked eye. Ejection of the beam was performed by carefully loosening the die set triaxially to avoid such failures.

2.2. Holographic setup

A geometric setup of the cantilever bending method for double-exposure holographic interferometry is presented in Fig. 1. For holographic exposures, a ruby laser (JK Lasers 2000, UK) having a wavelength of 694 nm, pulse energy of 1.2 J and pulse duration of the order of 10 ns, was used. The laser beam was split in two parts, the reference beam falling via mirrors directly on the Agfa Gevaert 10 E 75 photographic plate; the object beam was directed via mirrors to the sample surface, from where it was scattered to the photographic plate (Fig. 1). In the present case, the reference and the scattered laser beams were oriented perpendicularly to the sample beam setup.

2.3. Sample beam setup

A sample beam was fixed to one end of a stand with a clamp, while noting the known direction of compression during beam preparation (Fig. 2). The clamp, covering a distance of 10 mm at the fixed end of the beam, produced a constant pressure of 63.8 kPa perpendicular to the test beam surfaces. The optical setup for double-exposure holographic interferometry was arranged in such a way that the images of the upper and lower surfaces of the sample beam were recorded simultaneously. Bending load was generated by weights to the free end of the beam.

2.4. Holographic exposures

Double-exposure holographic measurement was accomplished by recording of two separate exposures on to the same photographic plate. Since both exposures appear in coherent light, and exist at approximately the same location in three-dimensional space, they interfere with each other and produce fringes overlying the reconstructed hologram. In this case, the disturbance causing the interference was generated by weights at the free end of the beam between exposures. With laser light, a reconstructed double-exposure hologram is formed with two overlapping wavefronts, resulting a typical fringe pattern corresponding to the exposures before and after adding the weight (Fig. 3). The reconstructed images were viewed on a monitor through an image processing system (i.e. a PC-computer, a gray level framegrabber and a CCD camera). By adjusting the camera position (i.e. the direction of viewing), the holographic images were captured, and the fringe positions on the images of the sample beams were marked using the computer's mouse and stored for further evaluation.

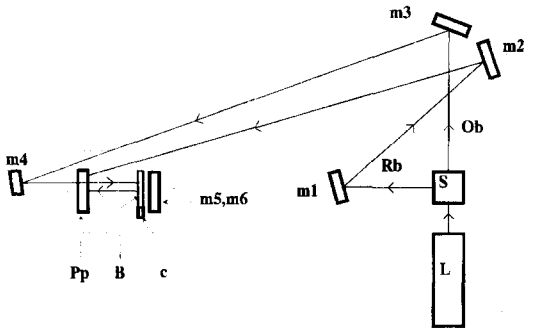

Fig. 1. A top view of the double-exposure holographic setup. L is the laser, S the laser beamsplitter, m1–m6 the mirrors, Pp the photographic plate, Ob and Rb the object and reference laser beams, respectively, and c the clamp holding sample beam B. The area inside the dotted line is the sample beam setup illustrated in Fig. 2.

A bright fringe was obtained when the phase shift between these two wavefronts was a multiple of 2π. This phase shift was caused by the change in optical path length due to bending, which was twice the vertical displacement at point x on the sample beam. If the displacement was D_x, then the corresponding phase shift was $(2D_x/\lambda)2\pi$, where λ is the laser wavelength. Furthermore, at the fixed end of the sample beam, the phase shift was zero and for the successive bright fringes 2π, 4π, etc. (Vest, 1979). Thus, for the nth bright fringe:

$$D_x = \frac{n\lambda}{2} \tag{1}$$

Using Eq. (1), where D_x is a function of the sample beam length, the elastic properties of the samples could be calculated for the lower and upper surfaces of the sample beam. More detailed descriptions of producing interference fringes, in the case of bending long-shaped objects by using external weights, have been reported by Silvennoinen et al., 1994a,b). In these studies, deflections interpreted from fringe spacing data, taken for sagittal and lateral observation, were experimentally verified.

2.5. Evaluation of bending

The bending properties as modulus values, E, were described separately for the upper and lower surfaces of the sample beams as a tensile and compressive modulus values, respectively. Values were calculated using a value of maximum displacement, D, with the equation of Young's modulus for cantilever bending:

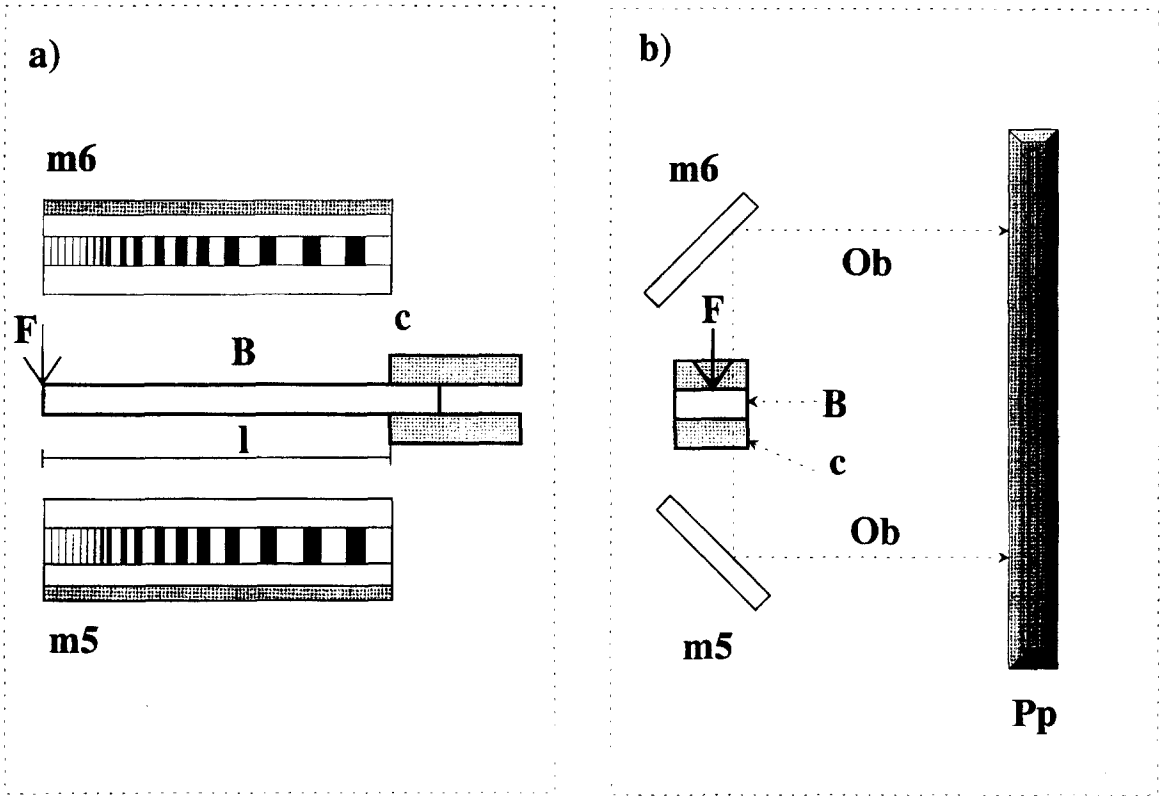

Fig. 2. A front (a) and a side view (b) of the sample beam setup. B is the sample beam, m5 and m6 the mirrors, F the bending force, l the beam length under bending, Ob the object laser beam, Pp the photographic plate and c the clamp holding the sample beam with a pressure of 63.8 kPa.

$$E = \frac{4\,Fl^3}{Dbh^3} \tag{2}$$

where F is the bending force, l is the length of the beam, h is the thickness and b is the width of the beam. The bending profiles, D_{bx} (i.e. the calculated theoretical displacement as a function of a beam length), were calculated using the following equation:

$$D_{\mathrm{bx}} = \frac{2Fl^3}{Ebh^3}\left[2 - 3\frac{x}{l} + \frac{x^3}{l^3}\right] \tag{3}$$

where D_{bx} is the displacement at point x on the beam. Calculations were performed assuming the modulus value to be the same along the beam length, obtained from Eq. (2). These bending profile analyses can be considered as an evaluation of both the cantilever bending method and, of course, the sample beams themselves. Extrapolation to zero porosity was made exponentially according to Spriggs-equation (Eq. (4)) (Spriggs, 1961):

$$E = E_0 \exp(-cP) \tag{4}$$

where E_0 is modulus value at zero porosity, c is constant and P is sample beam porosity.

2.6. Bending measurements

The weight-induced bending created a different number of fringes for the different materials. For further evaluation of the holograms, an appropriate number of fringes was maintained to ensure clear interpretation of bending. If the number of fringes had been very high, then limits of resolution would prevent adequate contrast for viewing holographic images. On the other hand, the num-

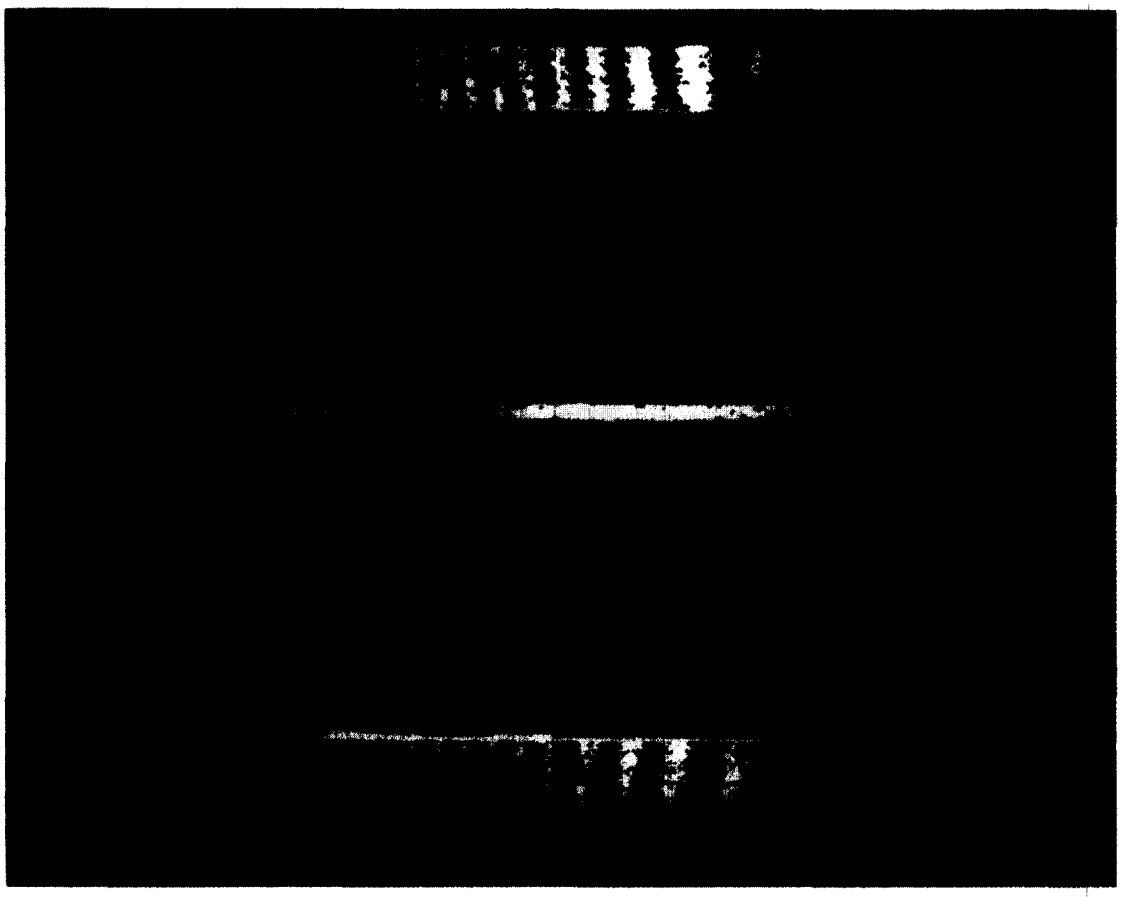

Fig. 3. A reconstruction of a double-exposure hologram recorded with a CCD camera of a microcrystalline cellulose beam under the preload of 0.0207 and the constant load of 0.00311 N.

ber of fringes had to be more than just a few to ensure an accurate bending analysis. To evaluate the appropriate size of the load sets to beam bending, and thus the appropriate number of resulting fringes, the bendings were initially examined with preloads of 0, 0.0207 and 0.0501 N for the first exposures, and then a constant load of 0.00311 N for the second exposures. Three parallel beam samples were selected approximately from the middle of the porosity range of each material. Porosities ($\pm$ S.E.) were 20.25 $\pm$ 0.90, 9.21 $\pm$ 0.43 and 21.21 $\pm$ 1.07% for dicalcium phosphate, microcrystalline cellulose and α-lactose, respectively. The bending profile analyses were made using the displacement data of the materials with every load set used.

Furthermore, the calculations of elastic moduli measurements were made in the elastic region of bending. To ensure that, and to evaluate the error of the holographic system, one dicalcium phosphate dihydrate beam (porosity 19.90%) was measured five times with a preload of 0.0207 N and a constant load of 0.00311 N. The time-gap between the two separate measurements was approximately 3 min. This amount of time was required to prepare a photographic plate for each new measurement.

To calculate the intrinsic material constant at zero porosity, five beams with different porosities were measured. Bendings were made by using a preload of 0.0207 N for the first exposures and a constant load of 0.00311 N for the second expo-

Table 1
The tensile and compressive modulus values (GPa ± S.D.) of materials for added preloads. The measurements were performed by adding a preload for the first holographic exposure, and a constant load of 0.00311 N for the second

	Preload/N					
	0		0.0207		0.0501	
Material	Tensile	Compressive	Tensile	Compressive	Tensile	Compressive
Microcrystalline cellulose	6.25 ± 0.02	6.38 ± 0.18	5.75 ± 0.38	5.78 ± 0.40	4.88 ± 0.36	5.03 ± 0.32
Dicalcium phosphate dihydrate	8.43 ± 0.70	8.30 ± 0.52	8.29 ± 1.54	8.34 ± 1.23	8.11 ± 0.89	8.36 ± 0.92
α-Lactose monohydrate	2.50 ± 0.48	2.61 ± 0.48	2.12 ± 0.46	2.13 ± 0.76	1.87 ± 0.33	1.96 ± 0.52

sures. This load set was found to be the most appropriate way to accurately interpret the elastic bending of materials, when considering the number of fringes obtained from beams of different porosities.

3. Results and discussion

Table 1 shows the tensile and compressive modulus values calculated from Eq. (2) for the preloads. A slight difference between the tensile and compressive modulus was detected with all materials, the compressive modulus being slightly bigger. The bending load was placed at the end of the beam on the upper surface, and some minor densification of the beam's structure was created. Thus, the upper surface bent slightly more than the lower surface and correspondingly, the compressive modulus values were slightly higher. In bending, with no preload (0 N), dicalcium phosphate showed an unexpected result in displaying a higher value for the tensile modulus. Most probably the bending force was inadequate to properly bend the beam. On the other hand, dicalcium phosphate behaved ideally over the whole measuring range (i.e. the modulus results were the same despite the weight of the added preload). For the more ductile material, microcrystalline cellulose, the modulus values decreased slightly as the preload increased. Bending with higher preloads seemed to create permanent changes in the structure of the cellulose beam. α-Lactose monohydrate has been shown to possess a strong surface-texture behaviour under compression, especially at the surface layers of the compact (Kourula et al., 1985). Thus, crystal planes of α-lactose are preferentially oriented to form a more structured layer on the very surface of the compact. Inside the compact, a typical randomized and less oriented structure existed. Modulus values with higher loads differed from the results obtained using the lowest. With the smallest preload, especially, the surface structure possibly predominates the elastic bending and, with the two higher preloads, and the surface structure beginning to collapse, the inner structure of the α-lactose beams predominates the bending.

The number of fringes was found to be optimal at a preload of 0.0207 N with all materials, and thus it was selected for further evaluation of moduli. When bending with no preload at all, the visibility of fringes was almost as suitable as it was with the selected preload; however, not enough fringes were created to gain clear interpretation. One could not be sure of the adequate elastic bending, as seen in the bending results of dicalcium phosphate (Table 1). For the highest preload, the number of fringes was too high for accurate interpretation, especially with very porous beams. The preload itself was perhaps creating permanent changes to the structure of the beams, especially with very porous ones.

Eq. (3), which was used to calculate the bending profile, has been derived from the theoretical behaviour of the intact, typically hard, and solid specimens. Thus, it most probably does not correctly describe the bending of a biphasic disperse

powder-air compact. With this in mind, the profile analysis was used in this study only to explain the most obvious unpredictable bending behaviour. Stabilizing the beam with a clamp that compressed the sample at a point perpendicular to a pressure of 63.8 kPa (Fig. 2) also produced stress within the beam. It can be seen from Fig. 4 that the displacement of the fixed end increased slightly due to induced stresses, when compared with the theoretical displacement curve obtained from Eq. (3). The trend was similar with all

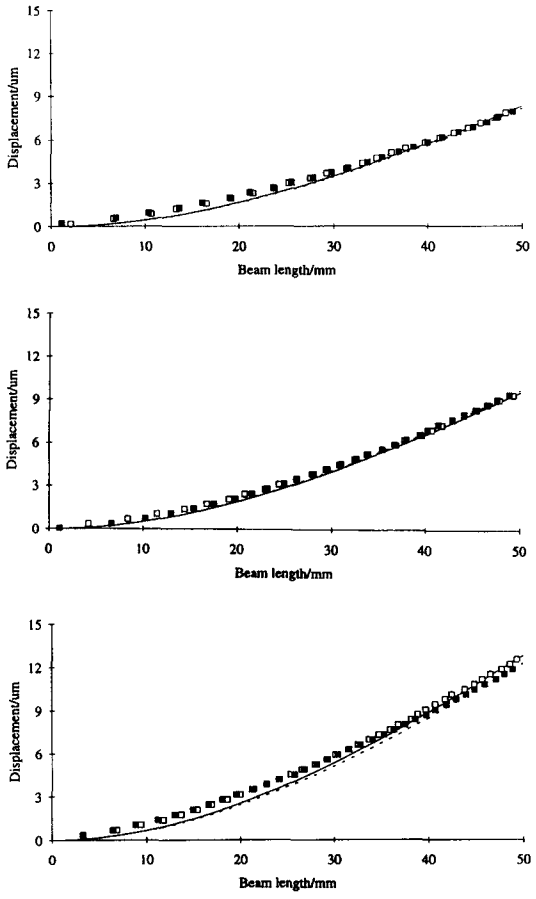

Fig. 4. The experimental displacement points and theoretical displacement curves for the materials used. Single marks indicate the experimental values and lines for the theoretical displacement curves. Open marks and solid lines represent the upper surfaces of beams, and closed marks and dotted lines the lower ones. a, b and c illustrate microcrystalline cellulose, dicalcium phosphate dihydrate and α-lactose monohydrate, respectively.

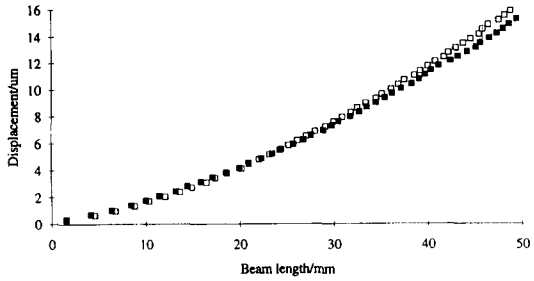

Fig. 5. The experimental displacement points of a α-lactose monohydrate beam under a preload of 0.0207 and a constant load of 0.00311 N. Open marks represent the upper surface and closed marks the lower surface of the beam.

preloads and all materials used. The irregularities in bending profiles revealed non-homogeneities in the structure of the specimen that were not so evidently visible to the naked eye, or observable by other conventional loading methods. This was seen with α-lactose beams which showed a structural deficiency by clearly illustrating a different bending of the upper and lower sides of the beam (Fig. 5). Besides heterogeneous structures, the stepwise collapse of the surface layer structures of α-lactose beams might also lead to this kind of behaviour under bending.

The error of the singular dicalcium phosphate beam, measured five times, was greatest at the free end of the beam, of the lower and upper surfaces, being ± 9.99% and ± 11.27%, respectively. Those bendings can be considered to exist in the linear portion of elasticity, since there was no trend of displacement to increase or decrease during measurement. The reported errors for double-exposure holographic measurements have been less than 2.3%, when covering a displacement range from 0 to 40 μm (Pryputniewicz and Bowley, 1978). Since the measured deviation was about 10%, when covering a displacement range from 0 to a maximum of 18 μm, most of the deviation was clearly caused by the sample beam setup (i.e. stabilization of the beam, and adding of the bending preload between measurements). As a result, the holographic system was considered to be measuring accurately.

The extrapolation results of dicalcium phosphate and microcrystalline cellulose are presented in Table 2. With both materials, the compressive

Table 2
Compressive and tensile modulus values (GPa) at zero porosity extrapolated with an exponential equation, where b is constant in the exponential equation, and r^2 is the correlation of the fit

Material	Compressive modulus	b	r^2	Tensile modulus	b	r^2
Microcrystalline cellulose	7.27	0.0502	0.9463	7.21	0.0511	0.9426
Dicalcium phosphate dihydrate	105.30	0.1350	0.9551	102.91	0.1344	0.9633

modulus values were slightly higher. These results were in good agreement with previously published results (Bassam et al., 1990). Unfortunately, with α-lactose, there were not enough successful bendings for reliable measurements, due to lamination of the sample beams. The lack of integrity was very clearly demonstrated in their holograms. With conventional displacement detecting methods, this lack of integrity would not had been noticed. A good example is seen in Fig. 6, where a major curving and poor contrast of the fringes exists, indicating a lamination effect of the sample beam.

According to this study double-exposure holo-

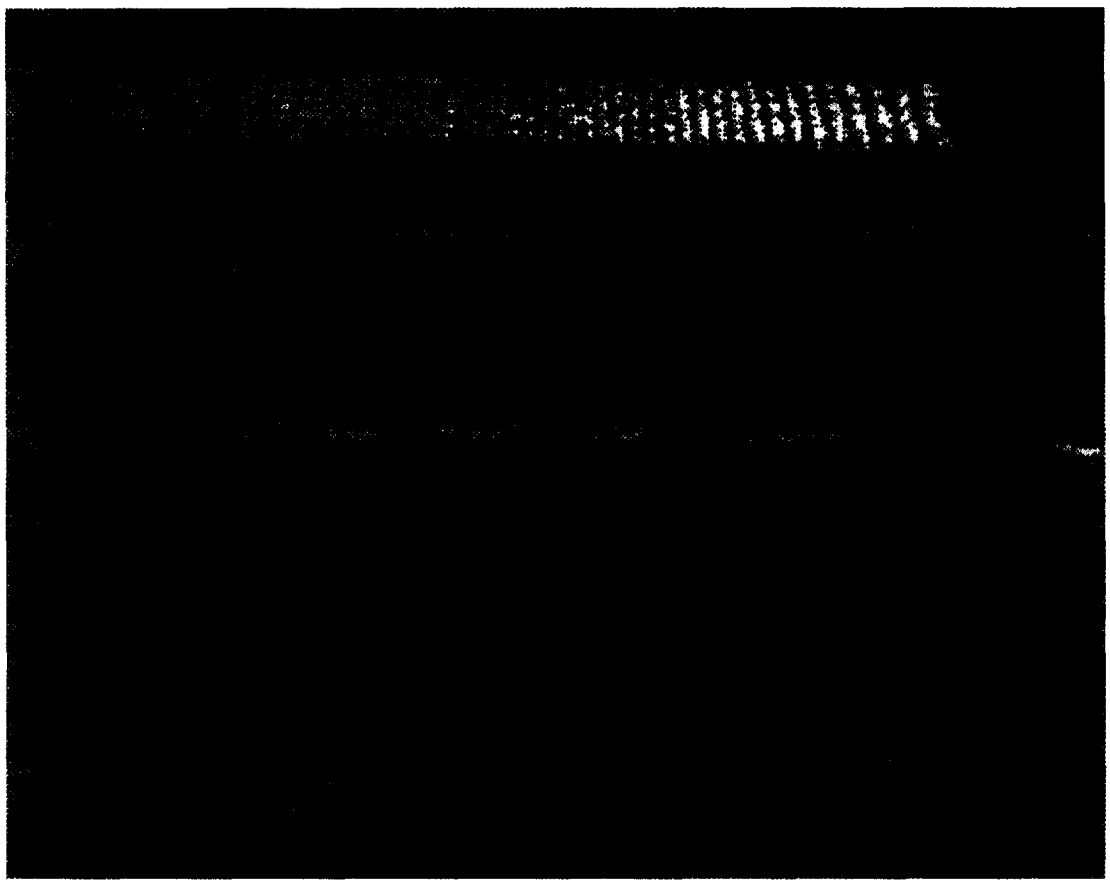

Fig. 6. Reconstruction of a α-lactose monohydrate beam. Poor contrast seen in the distal part of the beam illustrates structural defect.

graphic interferometry is a well suited, accurate and versatile method in the mechanical studies of pharmaceutical powders. Important benefits are the ease and reliability of evaluation for the bending profile along the whole beam, and not only a localized maximum displacement as typically measured by more conventional measuring devices. The most important benefit was the clear indication of integrity, or lack of integrity in pharmaceutical powder compacts, as demonstrated with α-lactose.

4. Unlinked references

Paronen and Juslin (1983), Roberts and Rowe (1987), Roberts et al. (1994), Svelto (1982)

References

Bassam, F., York, P., Rowe, R.C. and Roberts, R.J., Effect of particle size and source on variability of Young's modulus of microcrystalline cellulose powders. *J. Pharm. Pharmacol.*, 40 Suppl. (1988) 68.

Bassam, F., York, P., Rowe, R.C. and Roberts, R.J., Young's modulus of powders used as pharmaceutical excipients. *Int. J. Pharm.*, 64 (1990) 55–60.

Bassam, F., York, P., Rowe, R.C. and Roberts, R.J., The Young's modulus of binary powder mixtures. *Powder Technol.*, 65 (1991) 103–111.

Church, M.S. and Kennerley, J.W., An evaluation of four-point bending for the mechanical characterization of compacted pharmaceutical materials. In Rubinstein, M.H. (Ed.), Proceedings of the 4th Pharmaceutical Technology Conference, Edinburgh, Vol. 1, Solid Dosage Research Unit, Liverpool, UK, 1984, pp. 185–215.

Dhir, S.K. and Sikora, P., An improved method for obtaining the general-displacement field from a holographic interferogram. *Exp. Mech.*, 12 (1972) 323–327.

Dwivedi, S.K., Oates, R.J. and Mitchell, A.G., Estimation of elastic recovery, work of decompression and Young's modulus using a rotary tablet press. *J. Pharm. Pharmacol.*, 44 (1992) 459–466.

Holman, L.E. and Leuenberger, H., The relationship between solid fraction and mechanical properties of compacts: the percolation theory model approach. *Int. J. Pharm.*, 46 (1988) 35–44.

Kourula, J., Laine, E. and Paronen, P., Tablet hardness and texture measurements. *Dosis*, 1 (1) (1985) 18–26.

Mashadi, A.B. and Newton, J.M., The characterization of the mechanical properties of microcrystalline cellulose: a fracture mechanics approach. *J. Pharm. Pharmacol.*, 39 (1987) 961–965.

Pryputniewicz, R.J. and Bowley, W.W., Techniques of holographic displacement measurement: an experimental comparison. *Appl. Opt.*, 17(11) (1978) 1748–1756.

Raatikainen, P., Pöntinen, T., Ilkka, J., Ketolainen, J. and Paronen, P., Critical evaluation of three point bending test for measuring Young's modulus of pharmaceutical powders. In Rubinstein, M.H. (Ed.), Proceedings of the 13th Pharmaceutical Technology Conference, Strasbourg, Vol 2, Solid Dosage Research Unit, Liverpool, UK, 1994, pp. 192–203.

Roberts, R.J. and Rowe, R.C., The Young's modulus of pharmaceutical materials. *Int. J. Pharm.*, 37 (1987) 15–18.

Roberts, R.J., Rowe, R.C. and York, P., The relationship between Young's modulus of elasticity of organic solids and their molecular structure. *Powder Technol.*, 65 (1991) 139–146.

Roberts, R.J., Rowe, R.C. and York, P., The measurement of the critical stress intensity factor (K_{IC}) using three point single edge notched beam (SENB) testing. *Int. J. Pharm.*, 91 (1993) 173–182.

Silvennoinen, R., Nygrén, K., Rouvinen, J. and Petrova, V., Bone structure studies with holographic interferometric nondestructive testing and x-ray methods. *Opt. Eng.*, 33(2) (1994a) 473–478.

Silvennoinen, R., Nygrén, K. and Mozerov M., Holographic nondestructive testing in bone growth disturbance studies. *Opt. Eng.*, 33(3) (1994b) 830–834.

Sinko, C.M., Smith, D.P. and Nixon, P.R., Mechanical characterization of hydroxypropyl methylcellulose: modulus determination from indentation loading profiles. *Int. J. Pharm.*, 81 (1992) 243–252.

Spriggs, R.M., Expression for effect on elastic modulus of polycrystalline refractory materials, particularly aluminium oxide. *J. Am. Ceram. Soc.*, 44 (1961) 628–629.

Vest, C.M., Holographic Interferometry. Wiley, New York, USA, 1979, pp. 114–115.